Compressibilities and Volume Fluctuations of Archaeal Tetraether Liposomes

Parkson Lee-Gau Chong,[†*] Michael Sulc,[‡] and Roland Winter[‡*]
[†]Department of Biochemistry, Temple University School of Medicine, Philadelphia, Pennsylvania; and [‡]Faculty of Chemistry, Physical Chemistry I, Biophysical Chemistry, Technical University of Dortmund, Dortmund, Germany

ABSTRACT Bipolar tetraether lipids (BTLs) are abundant in crenarchaeota, which thrive in both thermophilic and nonthermophilic environments, with wide-ranging growth temperatures (4–108°C). BTL liposomes can serve as membrane models to explore the role of BTLs in the thermal stability of the plasma membrane of crenarchaeota. In this study, we focus on the liposomes made of the polar lipid fraction E (PLFE). PLFE is one of the main BTLs isolated from the thermoacidophilic crenarchaeon *Sulfolobus acidocaldarius*. Using molecular acoustics (ultrasound velocimetry and densimetry), pressure perturbation calorimetry, and differential scanning calorimetry, we have determined partial specific adiabatic and isothermal compressibility, their respective compressibility coefficients, partial specific volume, and relative volume fluctuations of PLFE large unilamellar vesicles (LUVs) over a wide range of temperatures (20–85°C). The results are compared with those obtained from liposomes made of dipalmitoyl-L-α-phosphatidylcholine (DPPC), a conventional monopolar diester lipid. We found that, in the entire temperature range examined, compressibilities of PLFE LUVs are low, comparable to those found in gel state of DPPC. Relative volume fluctuations of PLFE LUVs at any given temperature examined are 1.6–2.2 times more damped than those found in DPPC LUVs. Both compressibilities and relative volume fluctuations in PLFE LUVs are much less temperature-sensitive than those in DPPC liposomes. The isothermal compressibility coefficient (β_T^{lipid}) of PLFE LUVs changes from 3.59×10^{-10} Pa^{-1} at 25°C to 4.08×10^{-10} Pa^{-1} at 78°C. Volume fluctuations of PLFE LUVs change only 0.25% from 30°C to 80°C. The highly damped volume fluctuations and their low temperature sensitivity, echo that PLFE liposomes are rigid and tightly packed. To our knowledge, the data provide a deeper understanding of lipid packing in PLFE liposomes than has been previously reported, as well as a molecular explanation for the low solute permeation and limited membrane lateral motion. The obtained results may help to establish new strategies for rational design of stable BTL-based liposomes for drug/vaccine delivery.

INTRODUCTION

Crenarchaeota are traditionally referred to as thermophilic archaea with optimal growth temperatures between 60 and 108°C (1). More studies that are recent have shown that crenarchaeota are also present in nonextreme environments such as soils, lakes, and pelagic areas (4–22°C) (2–4). Bipolar tetraether lipids (BTLs) are abundant in both thermophilic and nonthermophilic crenarchaeota (5,6), but not in bacteria and eukaryotes. In many cases, BTLs constitute ~90% of the total polar lipids in the crenarchaeota. The structures of BTLs are distinctly different from the structures of lipids found in bacteria and eukaryotes (5,7). To date, the structural and functional role of BTLs in the crenarchaeota over such a wide-ranging growth temperature (4–108°C) remains elusive.

Liposomes made of BTLs can serve as membrane models to explore the role of BTLs in the plasma membrane of crenarchaeota. However, in a given crenarchaeon, there are several different kinds of BTLs (7–9). To gain a better molecular understanding of BTL liposomes, it is of considerable interest to use a purified BTL component, rather than total BTL extracts from the archaea.

In this article, we shall focus on the polar lipid fraction E (PLFE), which is one of the main BTLs isolated from the thermoacidophilic crenarchaeon *Sulfolobus acidocaldarius* (10). PLFE is a mixture of calditolglycerocaldarchaeol (also termed glycerol dialkylcalditol tetraether, or GDNT) and caldarchaeol (also termed glycerol dialkylglycerol tetraether, or GDGT) (10–13) (see Fig. 1 and (14)). The GDNT component (~90% of total PLFE) contains phospho-*myo*-inositol on the glycerol end and β-glucose on the calditol end, whereas the GDGT component (~10% of total PLFE) has phospho-*myo*-inositol attached to one glycerol and β-D-galactosyl-D-glucose to the other glycerol skeleton. The nonpolar regions of these lipids consist of a pair of 40-carbon biphytanyl chains, each of which contains up to four cyclopentane rings. In aqueous solutions, PLFE can form multilamellar and unilamellar vesicles of varying sizes (from 65 nm to 100 μm) (15–17).

PLFE liposomes are remarkably stable against environmental stressors (reviewed in (7,14,18)). PLFE liposomes exhibit an unusually low temperature sensitivity of proton permeation and dye leakage (15,16,19). The size of PLFE liposomes remains unchanged for at least six months at 25–55°C (20). At high [Ca^{2+}] (>12 mM), aggregation of PLFE liposomes occurs, but it is accompanied by only

Submitted August 17, 2010, and accepted for publication September 30, 2010.

*Correspondence: roland.winter@tu-dortmund.de or pchong02@temple.edu

Editor: Heiko H. Heerklotz.

0006-3495/10/11/3319/8 $2.00

doi: 10.1016/j.bpj.2010.09.061

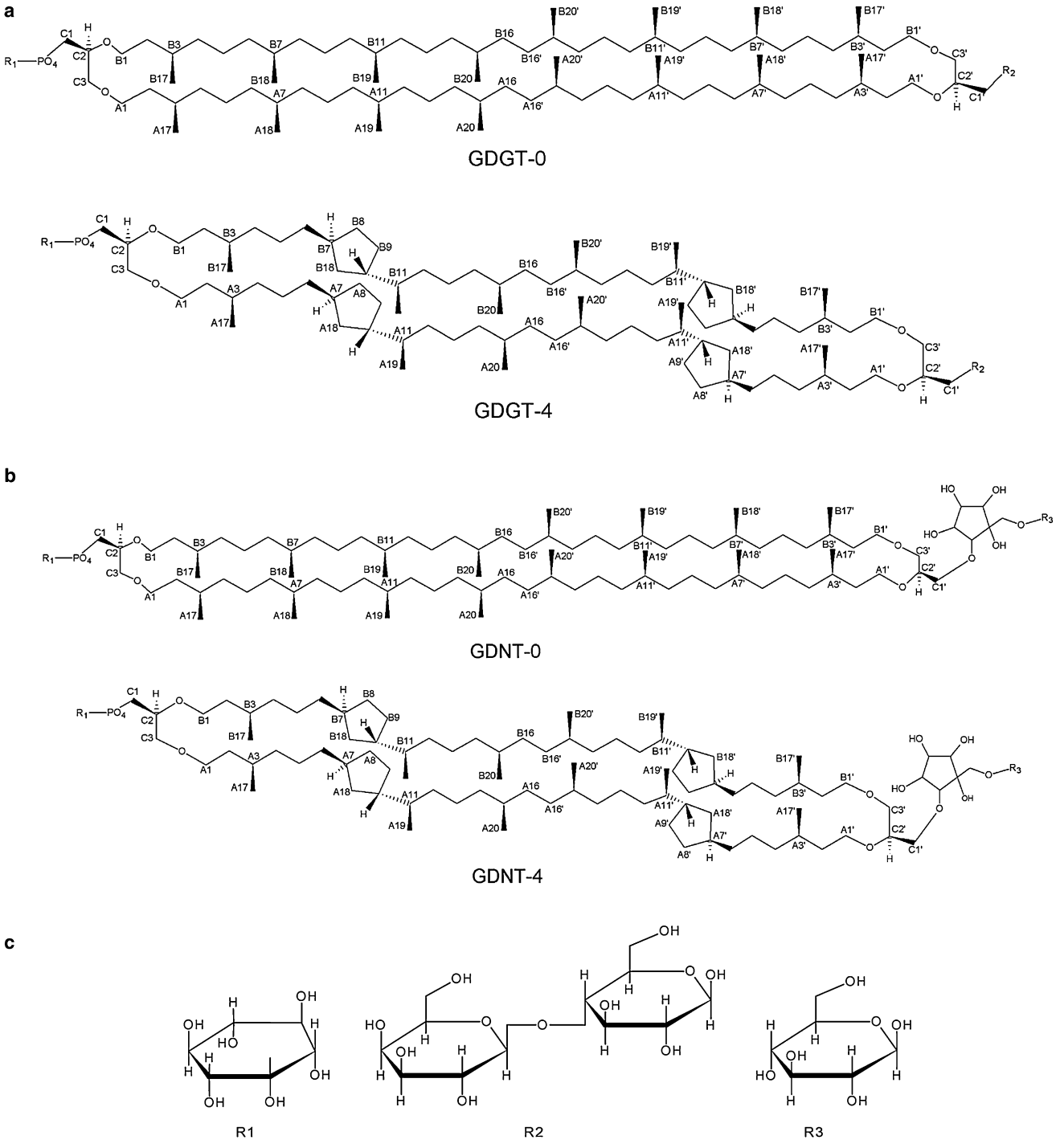

FIGURE 1 Bipolar tetraether lipids: molecular structures of (*a*) GDGT (or caldarchaeol) and (*b*) GDNT (or calditolglycerocaldarchaeol). GDG(N)T-0 and GDG(N)T-4 contain 0 and 4 cyclopentane rings, respectively. The number of cyclopentane rings in each biphytanyl chain can vary from 0 to 4 for the polar lipid fraction E (PLFE) derived from *S. acidocaldarius*. (*c*) Headgroups: R1 = myo-inositol; R2 = β-D-galactosyl-D-glucose; and R3 = β-D-glucose.

a relatively low extent of membrane fusion (20). The aggregation or fusion of PLFE liposomes is slow, on the order of tens of minutes (20–22), as compared to the aggregation of negatively charged monopolar diester liposomes at comparable Ca^{2+} and lipid concentrations (on the order of seconds) (23). PLFE liposomes also showed remarkable stability against autoclaving, displaying only 4.3% carboxyfluorescein leakage in the presence of 160 mM NaCl at pH 7.1 (24). In the pH range 4–10, PLFE-based liposomes are able to retain vesicle size and morphology through at least six autoclaving cycles (24). By contrast, at the same pH range, most conventional liposomes made of monopolar diester

lipids and cholesterol or pegylated lipids cannot withhold vesicle size against just one cycle of autoclaving (24).

The unusual stability of PLFE liposomes has been attributed in part to tight and rigid lipid packing as suggested by fluorescence probe techniques. For example, the generalized polarization values of Laurdan (6-lauroyl-2-(dimethylamino)naphthalene) fluorescence in PLFE giant unilamellar vesicles (GUVs) were low at all of the temperatures and pHs examined (17). When excited with light polarized in the *y* direction, Laurdan fluorescence in the center cross section of the PLFE GUVs exhibited a photoselection effect showing much-higher intensities in the *x*-direction of the vesicles, a result opposite that observed on monopolar diester liposomes. This surprising result indicates that the chromophore of Laurdan in PLFE GUVs is aligned parallel to the membrane surface. This photoselection effect and the low generalized polarization values suggest that the Laurdan chromophore resides in the polar headgroup region of the PLFE liposomes, whereas the lauroyl tail inserts into the hydrocarbon core of the membrane. This unusual L-shape disposition is presumably caused by the unique lipid structures and by the rigid and tight membrane packing in PLFE liposomes.

Packing tightness/rigidity in PLFE liposomes has also been studied by noninvasive methods such as pressure perturbation calorimetry (PPC). PPC data showed that all of the phase transitions of PLFE liposomes involve very small volume changes compared to the main transitions of saturated diacyl phosphatidylcholine bilayers (25). Note that PLFE liposomes may exhibit two thermally induced lamellar-to-lamellar phase transitions at ~42–50°C (varied with growth temperature and the pH used for the measurements) and ~60°C (7,17,25,26) and a lamellar-to-cubic phase transition at ~74–78°C (25,26).

In this study, we further investigate packing properties of PLFE liposomes with regard to volume changes. Specifically, we used molecular acoustics (ultrasound velocimetry and densimetry), PPC, and differential scanning calorimetry (DSC) to determine adiabatic and isothermal compressibility coefficients and volume fluctuations of PLFE liposomes as a function of temperature (22–82°C). Compressibilities and volume fluctuations of lipid membranes are not well documented in the literature.

To our knowledge, this work is the first study of isothermal compressibility coefficient and volume fluctuations of BTL liposomes. The results are compared with those obtained from liposomes made of dipalmitoyl-L-α-phosphatidylcholine (DPPC), a conventional monopolar diester lipid. We found that compressibilities of PLFE liposomes are low, comparable to those found in gel state of DPPC. Volume fluctuations of PLFE liposomes at any given temperature are much more damped than DPPC liposomes. Both compressibilities and volume fluctuations of PLFE liposomes are much less temperature-sensitive than those in DPPC liposomes. The data provide a deeper understanding of membrane packing and a molecular explanation for low solute permeation (15,16,19) and slow membrane dynamics (27,28) in PLFE liposomes. The obtained results may help to establish new strategies for rational design of thermally stable BTL-based liposomes for technological applications such as targeted drug delivery.

MATERIALS AND METHODS

Materials

Sulfolobus acidocaldarius cells (ATCC No. 49426; American Type Culture Collection, Rockville, MD) were grown aerobically and heterotrophically at 65°C and at pH 2.5–3.0. The cells were harvested before the stationary phase. PLFE lipids were isolated from dry cells as previously described (10,29). DPPC (dipalmitoyl-L-α-phosphatidylcholine) was purchased from Avanti Polar Lipids (Alabaster, AL).

Methods

Preparation of PLFE and DPPC liposomes

PLFE liposomes were prepared by dissolving PLFE lipids in chloroform/methanol/water (14:5:1, v/v/v), mixing the solution thoroughly using a vortex, and drying the solution first under a stream of nitrogen gas and then under high vacuum for at least 12 h. The lipid film was rehydrated with Millipore water (Purelab Classic; ELGA Labwater, Siershahn, Germany) followed by vortexing, sonication, and seven freeze/thaw cycles. Unilamellar vesicles (LUVs) were prepared by extrusion using a Mini-Extruder (Avanti Polar Lipids) and passing the solution 21 times through a 100-nm polycarbonate membrane at ~65°C. The final PLFE concentration used in the calorimetric, and density measurements, was 5 mg/mL. The PLFE concentration used in the ultrasound velocity measurements was 4 mg/mL. PLFE is a mixture of GDGT (glycerol dialkylglycerol tetraether) and GDNT (glycerol dialkylcalditol tetraether) containing varying numbers of cyclopentane rings. For simplicity, all the calculations performed in this study used a single molar weight of 2300 g for one mole of PLFE. DPPC LUVs were prepared by the same extrusion method.

Differential scanning calorimetry

Differential scanning calorimetry (DSC) measurements were made with a VP DSC calorimeter from MicroCal (Northampton, MA). The sample cell of the calorimeter was filled with ~0.5 mL of solution, with a lipid concentration of 5 mg/mL, while the reference cell was filled with a matching aqueous solution. Both heating and cooling scans were made at a scan rate of 10°C/h. Before each heating scan, the vesicles were kept at the starting temperature for ~2 h. The heat capacity c_p values are given with respect to the reference cell.

Pressure perturbation calorimetry

Pressure perturbation calorimetry (PPC) measurements were performed on the same MicroCal calorimeter equipped with a MicroCal pressurizing cap. A nitrogen gas pressure of 5 bar was applied to the samples (5 mg/mL) during all PPC cycles (30,31). The effective scan rate was 10°C/h. Under the same experimental conditions, a set of reference sample-water and water-water measurements was carried out each time. For calculation of the relative volume changes, a partial specific lipid volume of 1 $cm^3\ g^{-1}$ was used.

Density measurements

Density measurements were performed on a densitometer (model No. DMA5000; Anton Paar, Graz, Austria), using the principle of mechanical

harmonic oscillator to obtain the densities of the solution (ρ) and the water (ρ_0) as a function of temperature. The partial specific volume (v^o) of the lipid vesicles can be calculated by the equation (provided that the lipid vesicle solution is sufficiently diluted):

$$v^o = \left(\frac{\partial v}{\partial n}\right) \cong \frac{1}{\rho_0} - \frac{\rho - \rho_0}{\rho_0 c}. \quad (1)$$

Here v is the specific volume (in mL/g), n is the number of solute molecules, and c is the specific lipid concentration (in g/mL) in the solution (32,33). In this and the subsequent equations, the subscript "0" and superscript "o" denote water and the lipid vesicles or the solutes, respectively. For the density measurements, the average heating scan rate is 8°C/h.

Ultrasound velocity measurements

Ultrasound velocity u was measured using a ResoScan apparatus (TF Instruments, Heidelberg, Germany) which generates standing waves at a resonance frequency (f_N) in a resonator with a distance D between the resonator plates with a fixed order number N:

$$u = \frac{2Df_N}{N}. \quad (2)$$

The velocity number $[u]$ is given by

$$[u] = \frac{(u - u_0)}{u_0 c}, \quad (3)$$

where u and u_0 are the ultrasound velocity of the solution and the water, respectively. The values u and u_0 were measured as a function of temperature using a heating scan rate of 10°C/h (32,33).

Determinations of compressibility

The propagating ultrasound wave depends on the density (ρ) and adiabatic compressibility coefficient (β_S) of the medium. In combination with the density and ultrasound velocity measurements, we can calculate the adiabatic compressibility coefficient (32–34):

$$\beta_s = \frac{1}{u^2 \rho}. \quad (4)$$

In a two-component system (lipid + buffer), the partial specific molar adiabatic compressibility (κ_S°) of the solute (i.e., lipid) is given by

$$\kappa_S^o = \left(\frac{\partial \kappa_S}{\partial n}\right) = \left(\frac{\partial v^o}{\partial p}\right)_S \cong \beta_{S,0}\left(2(v^o - [u]) - \frac{1}{\rho_0}\right), \quad (5)$$

where $\beta_{S,0}$ is the adiabatic compressibility coefficient of the solvent (i.e., buffer). The value κ_S° is related to the partial specific adiabatic compressibility coefficient (β_S^{lipid}) of the lipid through the partial specific volume of the lipid, v^o:

$$\kappa_S^o = v^o \beta_S^{\text{lipid}}.$$

The partial specific isothermal compressibility of the lipid (κ_T°) can be calculated from κ_S° according to the equation (32,33)

$$\kappa_T^o = \kappa_S^o + \frac{T\alpha_0^2}{\rho_0 c_{p,0}}\left(2\frac{\alpha^o v^o}{\alpha_0} - \frac{c_p^o}{\rho_0 c_{p,0}}\right). \quad (6)$$

The partial specific thermal expansion coefficient of the lipid (α^o) can be obtained from PPC measurements. The thermal expansion coefficient (α) is defined as

$$\alpha = E/V,$$

where E is the thermal expansion and V is the molar volume. The DSC measurement yields the heat capacity at constant pressure (c_p) over a wide temperature range. The partial specific heat capacity (c_p°) of the solute can be calculated according to

$$c_p^o = \frac{\Delta C_p}{m} + \frac{v^o}{v_0^o} c_{p,0}, \quad (7)$$

where $c_{p,0}$ is the partial specific heat capacity of the solvent (i.e., buffer), ΔC_p is the heat capacity change through a phase transition, and m is the molecular mass of the lipid. Analogous to the adiabatic compressibility coefficient, the isothermal compressibility coefficient of the lipid (β^T_{lipid}) is defined by

$$\beta^T_{\text{lipid}} = \kappa_T^o / v^o.$$

Determination of fluctuation parameters

From the partial specific volume (v^o) and isothermal compressibility (κ_T°), the square average of the volume fluctuations

$$\langle \Delta V^2 \rangle = RTK_T = RT\kappa_T^o M$$

and the relative volume fluctuations

$$\sqrt{\frac{\langle \Delta V^2 \rangle}{V^2}} = \sqrt{\frac{RT\beta_T^{\text{lipid}}}{Mv^o}}$$

can be calculated (34,35).

RESULTS AND DISCUSSION

This study reports, for the first time to our knowledge, the isothermal compressibility and volume fluctuations of archaeal BTL liposomes. These important thermodynamic properties are calculated from the data obtained from acoustic and calorimetric measurements as described in Materials and Methods.

The acoustic measurements alone yield interesting information about PLFE liposomes. The ultrasound velocity number ($[u]$) of PLFE LUVs decreases slightly with increasing temperature, from 0.075 mL/g at 20°C to 0.025 mL/g at 85°C (Fig. 2). In this plot, there is a small change of slope at ~40°C, which may reflect a lipid phase transition. In sharp contrast, DPPC LUVs exhibit a dramatic change of $[u]$ with temperature, changing from 0.1 mL/g at 20°C to −0.16 mL/g at 65°C. There is an abrupt biphasic change in $[u]$ at the main phase transition temperature (~41°C) of DPPC. The slopes of $[u]$ versus T for both the gel ($<$ 37°C) and liquid-crystalline ($>$ 45°C) state of DPPC are much greater than that for PLFE liposomes. The velocity number $[u]$ of PLFE liposomes is much less temperature-sensitive than that of DPPC.

In addition, $[u]$ changes little through the phase transitions of PLFE liposomes, in sharp contrast to the abrupt change of $[u]$ through the main phase transition of DPPC. The

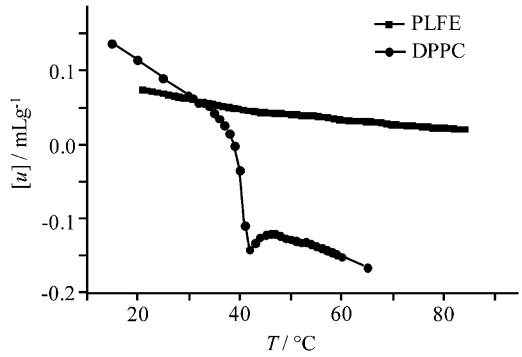

FIGURE 2 Temperature dependence of the ultrasound velocity number ([u]) of PLFE (*squares*) and DPPC (*circles*) liposomes.

[u]-versus-T profile for DPPC (Fig. 2) is similar to that previously reported, which is typical for a pseudo-first-order kind of phase transition (35–37). Fig. 2 also shows that PLFE and DPPC vesicles have the same ultrasound velocity number at ~30°C, which implies that, at this temperature, molecular packing in both membranes is approximately the same. The equivalence at this temperature propagates to the compressibility data shown later in Figs. 5 and 6. Further, in the temperature range examined, the velocity number for PLFE is always positive, while that for DPPC becomes negative at the phase transition. According to Eq. 3, [u] is positive when the ultrasound velocity of the liposomes (u) is greater than that of water (u_0). This result indicates that the intermolecular interactions and molecular packing in PLFE liposomes remain strong and tight and change relatively little with temperature from 20 to 85°C.

The heat capacity (c_p) of PLFE LUVs measured from DSC exhibits an endothermic transition at ~40°C (Fig. 3). This transition temperature agrees with the break-point shown in the plot of [u] versus temperature (Fig. 1) and with the DSC data of PLFE MLVs (25). Our previous study (25) has shown that the enthalpy changes of the phase transitions in PLFE liposomes are small, compared to that in saturated diacyl phosphatidylcholines. The partial specific heat capacity (c_p°), which is calculated from Eq. 7, also shows a small but abrupt change at ~40°C (Fig. 3). These data echo the previous finding that ultrasound velocity number and heat capacity are strongly correlated (35,37,38).

The effect of temperature on the thermal expansion coefficient (α) of PLFE LUVs measured from PPC is presented in Fig. 4 (*top*). The data are more scattered and the peak is broader and shifted to a lower temperature, compared to our previous thermal expansion coefficient data obtained from PLFE MLVs (25). The differences may be attributed to the use of LUVs, which have less cooperativity in the phase transition than MLVs.

The temperature dependence of the partial specific volume (v^o) of PLFE liposomes is presented in Fig. 4 as well (*bottom*). There is a small change in slope at ~35°C (Fig. 4, *bottom*). This break-point matches with the weak transition at the similar temperature detected by PPC (Fig. 4, *top*). Above 35°C, the v^o value increases almost linearly with increasing temperature until ~78°C, which corresponds to the transition temperature from the lamellar to the cubic phase (26). Previous studies showed that PLFE liposomes exhibit two thermally induced lamellar-to-lamellar phase transitions at ~42–50°C (varied with cell growth temperature and the pH used for the measurements) and ~60°C (7,17,25,26). Our data (Fig. 4) indicate that there is a very small change in v^o near the first lamellar-to-lamellar phase transition and that there is virtually no change in v^o for the second lamellar-to-lamellar transition.

In sharp contrast, v^o of DPPC MLVs changes abruptly at the main phase transition, changing from 0.93 mL g^{-1} at 38°C to 0.98 mL g^{-1} at 42°C (33). The slope of v^o versus temperature (<78°C) for PLFE liposomes is ~0.00062 mL g^{-1} K^{-1} (Fig. 4). This value is comparable to the v^o variation with temperature in the gel state of DPPC MLVs but much smaller than that for the liquid-crystalline state of DPPC (0.00109 mL g^{-1} K^{-1}, estimated from Fig. 3 of (33)). These results imply that the temperature dependence of membrane packing in PLFE liposomes is similar to that

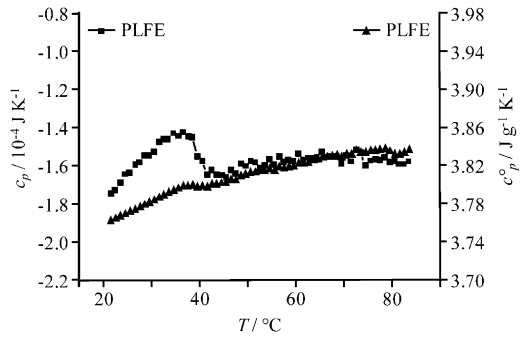

FIGURE 3 Effect of temperature on the heat capacity (c_p, *squares*) and partial specific heat capacity (c°_p, *triangles*) of PLFE liposomes. The heat capacity was determined by DSC using a heating mode. [PLFE] = 5 mg/mL.

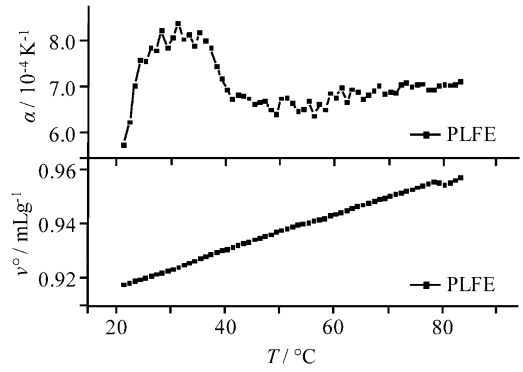

FIGURE 4 Temperature dependence of the thermal expansion coefficient (α) (*top*) and partial specific volume (v^o) (*bottom*) of PLFE liposomes. [PLFE] = 5 mg/mL.

found in the gel state of DPPC, but unlike that in liquid-crystalline state of DPPC.

Fig. 5 shows how the partial specific adiabatic compressibility (κ_S°) of PLFE LUVs (*squares*) and DPPC LUVs (*circles*) varies with temperature. The κ_S° of DPPC LUVs undergoes a dramatic increase at the main phase transition temperature (~41°C), yielding a change of ~1.9 × 10^{-10} mL g^{-1} Pa^{-1} over the 5° transition temperature span. In sharp contrast, κ_S° of PLFE LUVs changes almost linearly with increasing temperature and changes very little over a wide temperature range (21–83°C). Specifically, κ_S° of PLFE LUVs changes 0.008 × 10^{-10} mL g^{-1} Pa^{-1} per degree. The κ_S° for PLFE LUVs is much less temperature-sensitive than that for the gel or liquid-crystalline state of DPPC LUVs. The values of κ_S° for PLFE LUVs in the entire temperature range examined are low, close to the κ_S° values for the gel state of DPPC.

Similar results were obtained for the partial specific isothermal compressibility (κ_T°) (Fig. 6), despite that, as expected, the values of κ_T° are slightly higher than those of κ_S°. The value κ_T° also changes little with temperature, with an average change of 0.013 × 10^{-10} mL g^{-1} Pa^{-1} per degree. The plot of κ_T° versus temperature (Fig. 6) shows a small deviation from linearity at 37–45°C, which corresponds to one of the lamellar-to-lamellar phase transition temperatures of PLFE LUVs (7,17,25,26). The values of the isothermal compressibility coefficient (β^T_{lipid}) (calculated by $\beta^T_{\text{lipid}} = \kappa_T^\circ/\nu^\circ$) for PLFE LUVs at different temperatures are given in Table 1. These values are comparable to the β^T_{lipid} values for the gel state of DPPC (5.2 × 10^{-10} Pa^{-1} (39); 2.3 × 10^{-10} Pa^{-1} (35); 3.8 × 10^{-10} Pa^{-1} (33); and 4.2 × 10^{-10} Pa^{-1} (40)). The temperature dependence of β^T_{lipid} for PLFE LUVs is ~0.0092 × 10^{-10} Pa^{-1} K^{-1} (estimated from Table 1).

The most striking result lies in the relative volume fluctuations

$$\left(\langle \Delta V^2 \rangle / V^2\right)^{1/2},$$

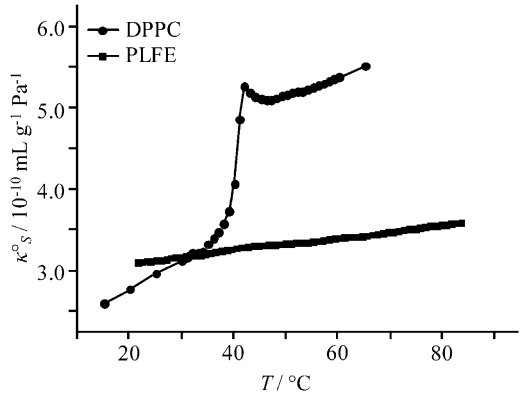

FIGURE 5 Temperature dependence of partial specific adiabatic compressibility (κ_S°) of PLFE (*squares*) and DPPC (*circles*) LUVs. [PLFE] = [DPPC] = 5 mg/mL.

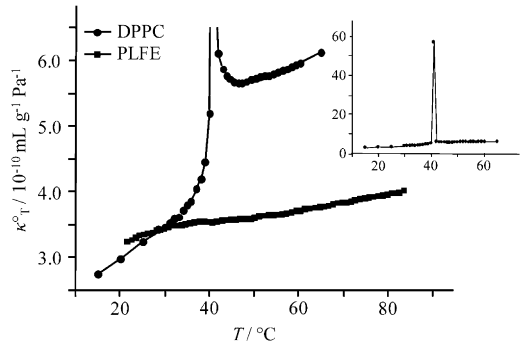

FIGURE 6 Temperature dependence of the partial specific isothermal compressibility (κ_T°) of PLFE (*squares*) and DPPC (*circles*) LUVs. (*Inset*) The full profile of the partial specific isothermal compressibility of DPPC LUVs. [PLFE] = [DPPC] = 5 mg/mL.

(Fig. 7), which can be calculated from the isothermal compressibility data. The relative volume fluctuations for DPPC LUVs are higher than those for PLFE LUVs by a factor of 1.6–2.2 at any given temperature examined. In addition, relative volume fluctuations of PLFE LUVs change only 0.25% from 30°C to 80°C. Relative volume fluctuations are closely related to solute permeation across lipid membranes and lateral motions of membrane components (41,42). Thus, the low values for relative volume fluctuations explain why PLFE liposomes exhibit an unusually low value and low temperature sensitivity to proton permeation and dye leakage (15,16,19) and limited lipid lateral motion in the membrane (17,27).

There is a small but noticeable slope change at ~39°C in the plot of $(\langle \Delta V^2 \rangle / V^2)^{1/2}$ versus temperature (Fig. 7). This slope change corresponds to a known lamellar-to-lamellar phase transition of PLFE liposomes at ~42–50°C (7,17,25,26), in good agreement with the [u], c_p, and ν^o data mentioned earlier. It appears that this phase transition does not involve a large change in relative volume fluctuations, which might be expected for lamellar phase transitions with minor changes in the chain packing density.

The highly damped volume fluctuations and their low temperature sensitivity are consistent with the concept that bipolar tetraether liposomes are rigid and tightly packed over a wide temperature range. Because the bipolar tetraether lipids are the major lipid component in crenarchaeota, our present finding may provide a partial explanation as to why crenarchaeota can sustain a wide range of growth temperature 4–108°C (as mentioned earlier).

TABLE 1 The isothermal compressibility coefficient of PLFE (β_T^{lipid}) determined at different temperatures

Temperature / °C	β_T^{lipid} (10^{-10} Pa^{-1})
25	3.59
40	3.76
53	3.83
67	3.95
78	4.08

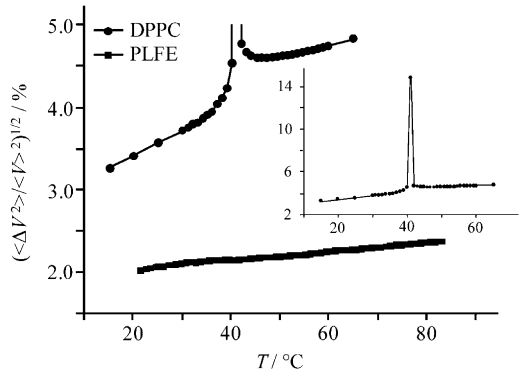

FIGURE 7 Temperature dependence of relative volume fluctuations $(\langle\Delta V^2\rangle/V^2)^{1/2}$ in PLFE (*squares*) and DPPC (*circles*) LUVs. (*Inset*) The data of DPPC LUVs presented in a larger scale. [PLFE] = [DPPC] = 5 mg/mL.

It is interesting to note that, even in this kind of tough membrane environment, a few proteins, including a leucine transport system, cytochrome-*c* oxidase, quinol oxidase, primary proton pumps, and isoprenylcysteine carboxyl methyltransferase, can still insert into the lipid matrix and remain biochemically active (43–48). In the future, it would be of interest to investigate the way in which protein insertion affects volume fluctuations of PLFE liposomes. It would also be important to study the changes in protein conformation that occur when the proteins insert into the tightly-packed PLFE lipid matrix.

In addition, liposomes made of either natural or synthetic BTL can be used for technological applications. A considerable effort has been devoted to develop BTL or BTL-containing liposomes as carriers of therapeutic agents and as adjuvants of drugs and vaccines (49–52). A full thermodynamic characterization of the PLFE membranes such as presented in this study may help to establish new strategies for rational design of thermally and biochemically stable BTL-based liposomes for targeted delivery and controlled release of drugs/vaccines.

The authors gratefully acknowledge support from the National Science Foundation (grant No. DMR-0706410), the Deutsche Forschungsgemeinschaft, the BMBF, and the country Northrhine-Westfalia (Europäischer Fonds für regionale Entwicklung).

REFERENCES

1. Woese, C. R., O. Kandler, and M. L. Wheelis. 1990. Towards a natural system of organisms: proposal for the domains *Archaea, Bacteria*, and *Eucarya*. *Proc. Natl. Acad. Sci. USA.* 87:4576–4579.
2. DeLong, E. F. 1992. Archaea in coastal marine environments. *Proc. Natl. Acad. Sci. USA.* 89:5685–5689.
3. Fuhrman, J. A., K. McCallum, and A. A. Davis. 1992. Novel major archaebacterial group from marine plankton. *Nature.* 356:148–149.
4. Karner, M. B., E. F. DeLong, and D. M. Karl. 2001. Archaeal dominance in the mesopelagic zone of the Pacific Ocean. *Nature.* 409:507–510.
5. De Rosa, M., and A. Gambacorta. 1988. The lipids of archaebacteria. *Prog. Lipid Res.* 27:153–175.
6. Powers, L. A., J. P. Werne, …, S. Schouten. 2004. Crenarchaeotal membrane lipids in lake sediments: a new paleotemperature proxy for continental paleoclimate reconstruction? *Geology.* 33:613–616.
7. Gliozzi, A., A. Relini, and P. L.-G. Chong. 2002. Structure and permeability properties of biomimetic membranes of bolaform archaeal tetraether lipids. *J. Membr. Sci.* 206:131–147.
8. Schouten, S., E. C. Hopmans, …, J. S. Damste. 2000. Widespread occurrence of structurally diverse tetraether membrane lipids: evidence for the ubiquitous presence of low-temperature relatives of hyperthermophiles. *Proc. Natl. Acad. Sci. USA.* 97:14421–14426.
9. Pearson, A., Z. Huang, …, C. L. Zhang. 2004. Nonmarine crenarchaeol in Nevada hot springs. *Appl. Environ. Microbiol.* 70:5229–5237.
10. Lo, S. L., and E. L. Chang. 1990. Purification and characterization of a liposomal-forming tetraether lipid fraction. *Biochem. Biophys. Res. Commun.* 167:238–243.
11. Kates, M. 1992. Archaebacterial lipids: structure, biosynthesis and function. *In* The Archaebacteria: Biochemistry and Biotechnology. M. J. Danson, D. W. Hough, and G. G. Lunt, editors. Portland Press, London, UK. pp. 51–72.
12. Sugai, A., R. Sakuma, …, T. Itoh. 1995. The structure of the core polyol of the ether lipids from *Sulfolobus acidocaldarius*. *Lipids.* 30:339–344.
13. Koga, Y., and H. Morii. 2005. Recent advances in structural research on ether lipids from archaea including comparative and physiological aspects. *Biosci. Biotechnol. Biochem.* 69:2019–2034.
14. Chong, P. L.-G. 2010. Archaebacterial bipolar tetraether lipids: physico-chemical and membrane properties. *Chem. Phys. Lipids.* 163:253–265.
15. Chang, E. L. 1994. Unusual thermal stability of liposomes made from bipolar tetraether lipids. *Biochem. Biophys. Res. Commun.* 202:673–679.
16. Komatsu, H., and P. L.-G. Chong. 1998. Low permeability of liposomal membranes composed of bipolar tetraether lipids from thermoacidophilic archaebacterium *Sulfolobus acidocaldarius*. *Biochemistry.* 37:107–115.
17. Bagatolli, L. A., E. Gratton, …, P. L. Chong. 2000. Two-photon fluorescence microscopy studies of bipolar tetraether giant liposomes from thermoacidophilic archaebacteria *Sulfolobus acidocaldarius*. *Biophys. J.* 79:416–425.
18. Chong, P. L.-G. 2008. Physical properties of membranes composed of tetraether archaeal lipids. *In* Thermophiles. F. Robb, G. Antranikian, D. Grogan, and A. Driessen, editors. CRC Press, Boca Raton, FL. pp. 73–95.
19. Elferink, M. G., J. G. de Wit, …, W. N. Konings. 1994. Stability and proton-permeability of liposomes composed of archaeal tetraether lipids. *Biochim. Biophys. Acta.* 1193:247–254.
20. Kanichay, R., L. T. Boni, …, P. L. Chong. 2003. Calcium-induced aggregation of archaeal bipolar tetraether liposomes derived from the thermoacidophilic archaeon *Sulfolobus acidocaldarius*. *Archaea.* 1:175–183.
21. Relini, A., D. Cassinadri, …, A. Gliozzi. 1994. Calcium-induced interaction and fusion of archaeobacterial lipid vesicles: a fluorescence study. *Biochim. Biophys. Acta.* 1194:17–24.
22. Relini, A., D. Cassinadri, …, A. Gliozzi. 1996. Effect of physical constraints on the mechanisms of membrane fusion: bolaform lipid vesicles as model systems. *Biophys. J.* 71:1789–1795.
23. Sundler, R., and D. Papahadjopoulos. 1981. Control of membrane fusion by phospholipid head groups. I. Phosphatidate/phosphatidylinositol specificity. *Biochim. Biophys. Acta.* 649:743–750.
24. Brown, D. A., B. Venegas, …, P. L. Chong. 2009. Bipolar tetraether archaeosomes exhibit unusual stability against autoclaving as studied by dynamic light scattering and electron microscopy. *Chem. Phys. Lipids.* 159:95–103.

25. Chong, P. L.-G., R. Ravindra, …, R. Winter. 2005. Pressure perturbation and differential scanning calorimetric studies of bipolar tetraether liposomes derived from the thermoacidophilic archaeon *Sulfolobus acidocaldarius*. *Biophys. J.* 89:1841–1849.

26. Chong, P. L.-G., M. Zein, …, R. Winter. 2003. Structure and conformation of bipolar tetraether lipid membranes derived from thermoacidophilic archaeon *Sulfolobus acidocaldarius* as revealed by small-angle x-ray scattering and high pressure FT-IR spectroscopy. *J. Phys. Chem.* 107:8694–8700.

27. Kao, Y. L., E. L. Chang, and P. L.-G. Chong. 1992. Unusual pressure dependence of the lateral motion of pyrene-labeled phosphatidylcholine in bipolar lipid vesicles. *Biochem. Biophys. Res. Commun.* 188:1241–1246.

28. Khan, T. K., and P. L.-G. Chong. 2000. Studies of archaebacterial bipolar tetraether liposomes by perylene fluorescence. *Biophys. J.* 78:1390–1399.

29. Lo, S. L., C. E. Montague, and E. L. Chang. 1989. Purification of glycerol dialkyl nonitol tetraether from *Sulfolobus acidocaldarius*. *J. Lipid Res.* 30:944–949.

30. Dzwolak, W., R. Ravindra, …, R. Winter. 2003. Aggregation of bovine insulin probed by DSC/PPC calorimetry and FTIR spectroscopy. *Biochemistry.* 42:11347–11355.

31. Ravindra, R., and R. Winter. 2004. Pressure perturbation calorimetry: a new technique provides surprising results on the effects of co-solvents on protein solvation and unfolding behavior. *ChemPhysChem.* 5:566–571.

32. Chalikian, T. V. 2003. Volumetric properties of proteins. *Annu. Rev. Biophys. Biomol. Struct.* 32:207–235.

33. Krivanek, R., L. Okoro, and R. Winter. 2008. Effect of cholesterol and ergosterol on the compressibility and volume fluctuations of phospholipid-sterol bilayers in the critical point region: a molecular acoustic and calorimetric study. *Biophys. J.* 94:3538–3548.

34. Smirnovas, V., R. Winter, …, W. Dzwolak. 2005. Thermodynamic properties underlying the α-helix-to-β-sheet transition, aggregation, and amyloidogenesis of polylysine as probed by calorimetry, densimetry, and ultrasound velocimetry. *J. Phys. Chem. B.* 109:19043–19045.

35. Schrader, W., H. Ebel, …, U. Kaatze. 2002. Compressibility of lipid mixtures studied by calorimetry and ultrasonic velocity measurements. *J. Phys. Chem. B.* 106:6581–6586.

36. Agafonov, A. V., E. N. Gritsenko, …, G. D. Mironova. 2007. Ca^{2+}-induced phase separation in the membrane of palmitate-containing liposomes and its possible relation to membrane permeabilization. *J. Membr. Biol.* 215:57–68.

37. Oliynyk, V., M. Jäger, …, U. Kaatze. 2008. Lipid membrane domain formation and alamethicin aggregation studied by calorimetry, sound velocity measurements, and atomic force microscopy. *Biophys. Chem.* 134:168–177.

38. Halstenberg, S., T. Heimburg, …, R. Krivanek. 1998. Cholesterol-induced variations in the volume and enthalpy fluctuations of lipid bilayers. *Biophys. J.* 75:264–271.

39. Tosh, R. E., and P. J. Collings. 1986. High pressure volumetric measurements in dipalmitoylphosphatidylcholine bilayers. *Biochim. Biophys. Acta.* 859:10–14.

40. Seemann, H., and R. Winter. 2003. Volumetric properties, compressibility and volume fluctuations in phospholipid-cholesterol bilayers. *Z. Phys. Chem.* 217:831–846.

41. Falck, E., M. Patra, …, I. Vattulainen. 2004. Impact of cholesterol on voids in phospholipid membranes. *J. Chem. Phys.* 121:12676–12689.

42. Almeida, P. F., W. L. Vaz, and T. E. Thompson. 1992. Lateral diffusion and percolation in two-phase, two-component lipid bilayers. Topology of the solid-phase domains in-plane and across the lipid bilayer. *Biochemistry.* 31:7198–7210.

43. Elferink, M. G., J. G. de Wit, …, W. N. Konings. 1992. Functional reconstitution of membrane proteins in monolayer liposomes from bipolar lipids of *Sulfolobus acidocaldarius*. *J. Biol. Chem.* 267:1375–1381.

44. In't Veld, G., M. G. Elferink, …, W. N. Konings. 1992. Reconstitution of the leucine transport system of *Lactococcus lactis* into liposomes composed of membrane-spanning lipids from *Sulfolobus acidocaldarius*. *Biochemistry.* 31:12493–12499.

45. Elferink, M. G., J. G. De Wit, …, W. N. Konings. 1993. Energy-transducing properties of primary proton pumps reconstituted into archaeal bipolar lipid vesicles. *Eur. J. Biochem.* 214:917–925.

46. Freisleben, H. J., K. Zwicker, …, T. Nawroth. 1995. Reconstitution of bacteriorhodopsin and ATP synthase from *Micrococcus luteus* into liposomes of the purified main tetraether lipid from *Thermoplasma acidophilum*: proton conductance and light-driven ATP synthesis. *Chem. Phys. Lipids.* 78:137–147.

47. Febo-Ayala, W., S. L. Morera-Félix, …, D. H. Thompson. 2006. Functional reconstitution of the integral membrane enzyme, isoprenylcysteine carboxyl methyltransferase, in synthetic bolalipid membrane vesicles. *Biochemistry.* 45:14683–14694.

48. Elferink, M. G. L., T. Bosma, …, W. N. Konings. 1995. Thermostability of respiratory terminal oxidases in the lipid environment. *Biochim. Biophys. Acta.* 1230:31–37.

49. Patel, G. B., and G. D. Sprott. 1999. Archaeobacterial ether lipid liposomes (archaeosomes) as novel vaccine and drug delivery systems. *Crit. Rev. Biotechnol.* 19:317–357.

50. Whitfield, D. M., E. E. Eichler, and G. D. Sprott. 2008. Synthesis of archaeal glycolipid adjuvants—what is the optimum number of sugars? *Carbohydr. Res.* 343:2349–2360.

51. Benvegnu, T., G. Réthoré, …, D. Plusquellec. 2005. Archaeosomes based on novel synthetic tetraether-type lipids for the development of oral delivery systems. *Chem. Commun. (Camb.).* 44:5536–5538.

52. Patel, G. B., B. J. Agnew, …, G. D. Sprott. 2000. In vitro assessment of archaeosome stability for developing oral delivery systems. *Int. J. Pharm.* 194:39–49.